

# Effects of Nano-SiO<sub>2</sub> on Setting Time and Compressive Strength of Alkali-activated Metakaolin-based Geopolymer

Kang Gao<sup>1</sup>, Kae-Long Lin<sup>2,\*</sup>, DeYing Wang<sup>1</sup>, Hau-Shing Shiu<sup>2</sup>, Chao-Lung Hwang<sup>3</sup> and Ta-Wui Cheng<sup>4</sup>

<sup>1</sup>Department of Environmental and Material Engineering, Yan-Tai University, China

<sup>2</sup>Department of Environmental Engineering, National Ilan University, Ilan 26047, Taiwan

<sup>3</sup>Department of Construction Engineering, National Taiwan University of Science and Technology, Taiwan

<sup>4</sup>Department of Materials and Mineral Resources Engineering, National Taipei University of Technology, Taiwan

**Abstract:** This study presents a discussion on the effects of different solid-to-liquid (S/L) ratios (0.97 to 1.19) and nano-SiO<sub>2</sub> (NS) percentages (0% to 3%) on some properties of metakaolin (MK)-based geopolymers. The setting time and compressive strength were investigated. Mercury intrusion porosimetry, fourier transform infrared spectroscopy, and scanning electron microscopy were used to determine the microstructure of the samples. The results show that a MK-based geopolymer sample added 1% NS with the S/L ratio of 1.03 exhibits more strength and less porosity. Applying NS to the geopolymer enhances compactness and increases strength. Therefore, nanotechnology can be used to improve geopolymers.

**Keywords:** Geopolymer, metakaolin, nano-SiO<sub>2</sub>, solid-to-liquid ratio, compressive strength.

## 1. INTRODUCTION

Geopolymers are a novel type of high-performance cementitious material. In 1978, Davidovits introduced the term geopolymer, referring to mineral polymers resulting from geochemistry or geosynthesis [1]. Geopolymerization is a reaction that chemically integrates minerals from silico-aluminate sources. Sources of alumina and silica act as a precursor source that readily dissolves in an alkaline solution. They are synthesized by alkaline or silicate activation, which lends itself to geopolymerization [2]. A geopolymer consists of a 3D network gel polymerized by SiO<sub>4</sub> and AlO<sub>4</sub> tetrahedrons and is prepared using natural mineral or solid waste [3].

Compared to Portland cement, geopolymers require less energy consumption, emit less CO<sub>2</sub>, exhibit high early strength, shrink less, exhibit low permeability, are fire and acid resistant, and are durable [4-6]. These characteristics make geopolymers promising building, high-strength, immobilization of toxic waste, sealing, and temperature-resistant materials [7]. Preparing geopolymers is easier than preparing Portland cement. They do not require high temperatures to calcine or sinter, and the polymerization reaction can be conducted at room temperature. Almost no NO<sub>x</sub>, SO<sub>x</sub>, or CO is generated, and CO<sub>2</sub> emissions are low [8].

Criado *et al.* suggested that the activation rate and chemical composition of a reaction product depend on the particle size, chemical composition, and type of alumino-silicate source and the activator concentration [9]. Nanoparticles are particles between 1 and 100 nm that create volume and surface effects. Nanoparticles preparation, application, its size and surface effects offer many benefits, and they can be used to develop high-performance polymers [10]. Nanosynthesis technology has been applied widely to develop novel materials with better properties and to improve conventional material properties. Studies have been conducted on nanocoatings, high-strength structural materials, macromolecular-based nanocomposites, magnetic materials, optical materials, and bionic materials [11].

Recent studies have shown that nanoparticles such as colloidal NS (consisting of an amorphous silicon dioxide core with a hydroxylated surface) have a high surface area to volume ratio and the potential for tremendous chemical reactivity. Aly *et al.* showed that adding a small amount of NS (up to 3 wt. %) accelerates pozzolanic activity, improves workability, controls alkali-silica reaction, and enhances the strength and durability of concrete [12]. Erich *et al.* found that geopolymer mortars produced using alternative NS-based activators exhibited similar or better mechanical performance than those produced using conventional activators [13]. The previous studies have shown that NS can improve mechanical properties of the cement pastes. But there is little literature studies have shown NS influence on the geopolymers. Therefore, this study presents a discussion on the effects of different S/L ratios (0.97 to 1.19) and NS percent-

\*Address correspondence to this author at the Department of Environmental Engineering, National Ilan University, Ilan 26047, Taiwan; Tel: (886) 3-9357400; Ext 7579; Fax: (886) 3-9364277; E-mail: [kllin@niu.edu.tw](mailto:kllin@niu.edu.tw)

ages (0% to 3%) on some properties of MK-based geopolymers. Setting time and compressive strength were investigated. Mercury intrusion porosimetry (MIP), Fourier transform infrared spectroscopy (FTIR), and a scanning electron microscope (SEM) were used to determine the microstructure of the samples.

## 2. EXPERIMENTAL DETAILS

### 2.1. Materials

MK was calcined using kaolin at 650 °C for 3 h. The Na<sub>2</sub>SiO<sub>3</sub> solution was produced in Taiwan. The composition of MK was 29.5% SiO<sub>2</sub>, 9.1% Na<sub>2</sub>O, 61.4% H<sub>2</sub>O, and the Ms (SiO<sub>2</sub>/Na<sub>2</sub>O) was 3.4. Analytical-grade 99% pure NaOH was used. The NS used was a white powder. Table 1 shows that the SiO<sub>2</sub> content was 99.9%, the average particle size was approximately 10 nm, and the specific surface area was 670 m<sup>2</sup>/g. Fig. (1) shows the SEM image of the used NS.

The MK used in this study was obtained from kaolin calcined at 650 °C for 3 h. It was slightly pink. Before and after calcination, the specific gravity of kaolin and MK was 1.74 and 1.66, respectively. However, the pH values of kaolin and MK were 6.52 and 5.74, respectively. This is because dehydroxylation during calcination makes MK weakly acidic.

The chemical composition of raw materials was determined using X-ray fluorescence. The results show that kaolin is mainly composed of SiO<sub>2</sub> (53.7%) and Al<sub>2</sub>O<sub>3</sub> (37.88%). MK is composed of 59.6% SiO<sub>2</sub> and 38% Al<sub>2</sub>O<sub>3</sub>. Table 2 shows the chemical composition of the raw materials.

### 2.2. Mixture Preparation

NaOH and distilled water were mixed with a Na<sub>2</sub>SiO<sub>3</sub> solution and allowed to cool to room temperature. With constant stirring, NS was added to the alkali activator. The SiO<sub>2</sub>/Na<sub>2</sub>O ratio was 1.50; the S/L ratios were 0.97, 1.03, 1.10, and 1.19; and the nanosilica replacement levels were 0%, 1%, 2%, and 3%. The alkali activator solution was prepared 24 h before use to ensure that the activator component was mixed uniformly. Table 3 shows the mixture proportions. A mechanical mixer was used to mix the activator solution and 1000 g MK for a few minutes. The fresh paste was then rapidly poured into plastic molds (5 × 5 × 5 cm). Samples were placed into an oven at 80 °C for 24 h. Mechanical properties and the microstructure performance of specimens were tested after 1, 7, 14, 28 and 60 days.

### 2.3. Methods

1. Setting Time: The setting times of the fresh pastes were determined using a Vicat Needle following the standard procedure ASTM C191-08.
2. Compressive Strength: Compressive strength tests were performed after 1, 7, 14, 28 and 60 days using a 50 mm × 50 mm × 50 mm cubic sample, according to ASTM C109.
3. Mercury Intrusion Porosimetry (MIP): A Quantachrome Autoscan Mercury Intrusion Porosimeter was used, with intrusion pressures up to 60,000 psi. By using the

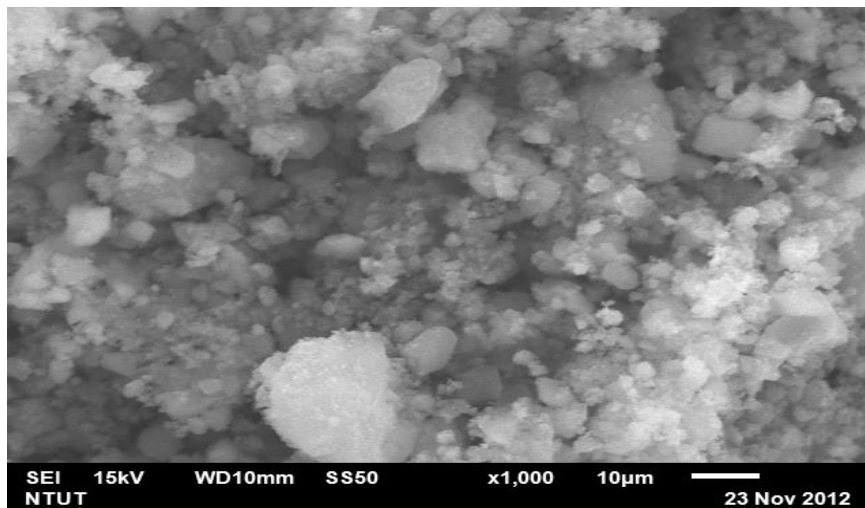


Fig. (1). SEM of nano-SiO<sub>2</sub>

Table 1. Properties of Nano-SiO<sub>2</sub>

Properties	Content of SiO <sub>2</sub> (%)	Phase			Compaction Density (g/cm <sup>3</sup> )	Average Particle size (nm)	Specific Surface Area(m <sup>2</sup> /g)
Content	99.9	Non-crystal white powder			0.14	10	670
Properties	Impurity (%)						
Content	Cl	Cu	Al	Ca	Fe	Mg	Sn
	0.028	0.003	0.002	0.002	0.001	0.001	0.001

**Table 2. Chemical Composition of Raw Materials**

Composition	Kaolinite	Metakaolin
SiO <sub>2</sub> (%)	53.70	59.60
Al <sub>2</sub> O <sub>3</sub> (%)	37.88	38.00
Fe <sub>2</sub> O <sub>3</sub> (%)	0.88	1.30
CaO (%)	0.20	0.24
MgO (%)	N.D.	N.D.
SO <sub>3</sub> (%)	N.D.	0.04
Na <sub>2</sub> O (%)	0.04	0.04
K <sub>2</sub> O (%)	0.34	0.32
LOI (%)	6.96	0.46

(N.D.,not detected)

**Table 3. Ratios of Material in Mixture**

S/L Ratios	NS Addition (%)	Mixture Proportion by Weight (g)				
		MK	NS	Na <sub>2</sub> SiO <sub>3</sub>	NaOH	H <sub>2</sub> O
0.97	0	1000	0	862.7	124.5	300
0.97	1	1000	10	862.7	124.5	300
0.97	2	1000	20	862.7	124.5	300
0.97	3	1000	30	862.7	124.5	300
1.03	0	1000	0	862.7	124.5	228.5
1.03	1	1000	10	862.7	124.5	228.5
1.03	2	1000	20	862.7	124.5	228.5
1.03	3	1000	30	862.7	124.5	228.5
1.10	0	1000	0	862.7	124.5	157
1.10	1	1000	10	862.7	124.5	157
1.10	2	1000	20	862.7	124.5	157
1.10	3	1000	30	862.7	124.5	157
1.19	0	1000	0	862.7	124.5	85.6
1.19	1	1000	10	862.7	124.5	85.6
1.19	2	1000	20	862.7	124.5	85.6
1.19	3	1000	30	862.7	124.5	85.6

Washburn equation,  $p = -\frac{2\gamma\cos\theta}{r}$ , the pore volume (V)

and the corresponding radius (r) were synchronously plotted by an X-T plotter, under the assumption that mercury wetting angle is  $\theta=140^\circ$ . In this equation, p,  $\gamma$ , r,  $\theta$ , stand for the applied pressure, surface tension, pore radius and wetting angle, respectively.

4. Chemical composition: The X-ray fluorescence (XRF) analysis was performed using an automated RIX 2000 spectrometer. Specimens were prepared for XRF analysis by mixing 0.4 g of sample and 4 g of 100 Spectroflux at a dilution ratio of 1:10. The homogenized mixtures were placed in Pt–Au crucibles before being heated for 1 h at 1,000°C in an electrical furnace. The homogeneous melted sample was recast into glass beads 2 mm thick and 32 mm in diameter.

- FTIR: Fourier transformation infrared spectroscopy (FTIR) was carried out on samples using the Elmer FTIR Spectrum L16000A Spectrometer and the KBr pellet technique (1 mg powdered sample mixed with 150 mg KBr).
- SEM: the microstructure of the geopolymer was studied using the electron beam from the Tescan Vega TS5136MM. For SEM analysis, samples were taken from specimens that had been fractured during compression testing and mounted in epoxy resin, polished and sputter coated with gold- palladium alloy. The samples were vacuum-dried overnight prior to SEM. The beam was applied at 10 KeV.

### 3. RESULTS AND DISCUSSION

#### 3.1. Setting Time

Fig. (2) shows the initial and final setting times of NS MK-based geopolymers with various S/L ratios. The initial and final setting times decreased significantly as the geopolymer S/L ratio increased. The initial setting times of 0%, 1%, 2%, and 3% NS samples at a S/L ratio of 0.97 were 315, 295, 277, and 240 min, and their final setting times were 375, 360, 330, and 285 min, respectively. This suggests that adding nanoparticles decrease the initial and final setting times. The setting time gradually decreased with the increase in NS content. This is because the surface effect, small size, high surface energy, and considerable scale of the atom located in the nanosilica surface are unique. Surface atoms

accelerate the system reaction rate because of their high activity and instability [14]. Lin *et al.* demonstrated that NS effectively reduced the setting time of sludge ash cement [15]. This is consistent with other results. The initial setting times of 0% NS pastes at S/L ratios of 0.97, 1.03, 1.1, and 1.19 were 315, 294, 289, and 225 min, and their final setting times were 375, 345, 330, and 285 min, respectively. This shows that setting time decreases as the S/L ratio increases. This reduces paste liquidity and decreases setting time.

#### 3.2. Compressive Strength

Fig. (3) shows the compressive strength of NS MK-based geopolymers at various S/L ratios. The results presented that the strength of geopolymers with different amounts of NS increased with curing time. With identical S/L ratios, the compressive strength of samples with different amounts of NS added was different. Geopolymers with various S/L ratios also showed significant differences. The Fig. (3) showed that the minimal compressive strength was obtained when the S/L ratio was 0.97.

Fig. (3) shows that the high compressive strength was obtained when the S/L ratio was 1.03. Early strength developed rapidly, and later strength developed steadily. When the amounts of 0%, 1%, 2%, and 3% NS were added, the compressive strength of geopolymers at 60 days were 43.7 MPa, 68.4 MPa, 59.5 MPa, and 49.2 MPa, respectively. This indicates that when the S/L ratio of MK-based geopolymers is 1.03, the optimal amount of NS is 1%.

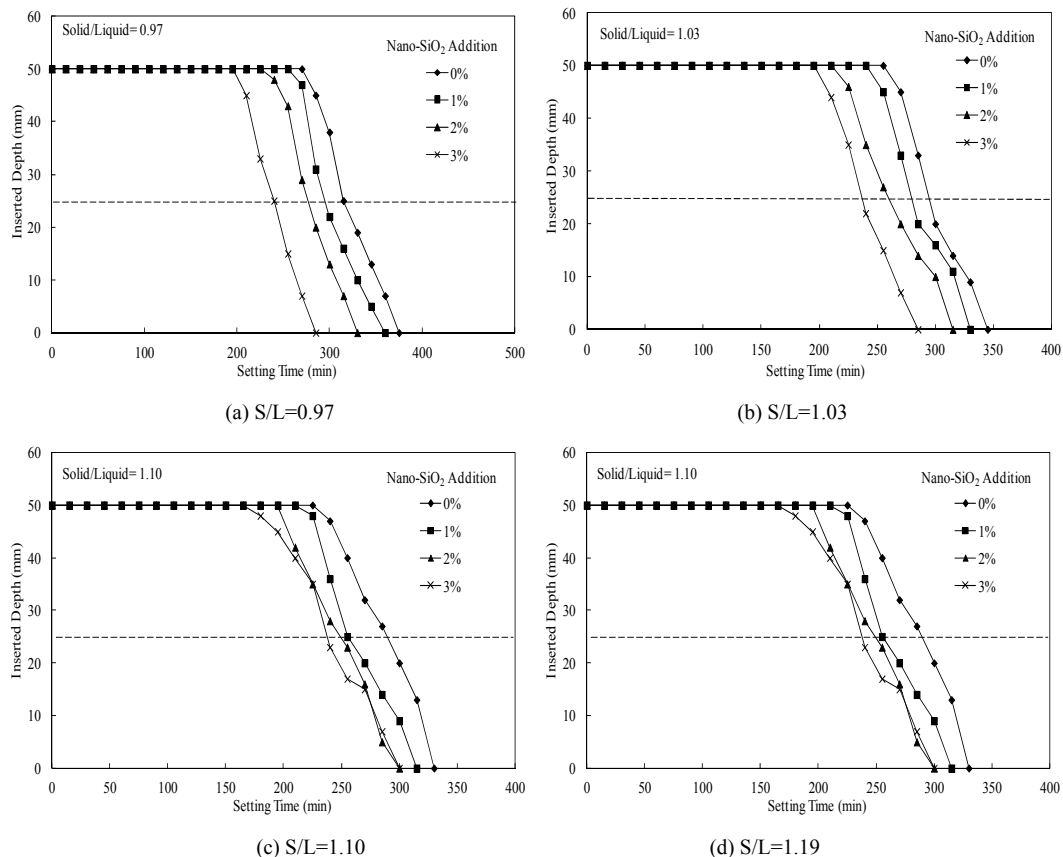
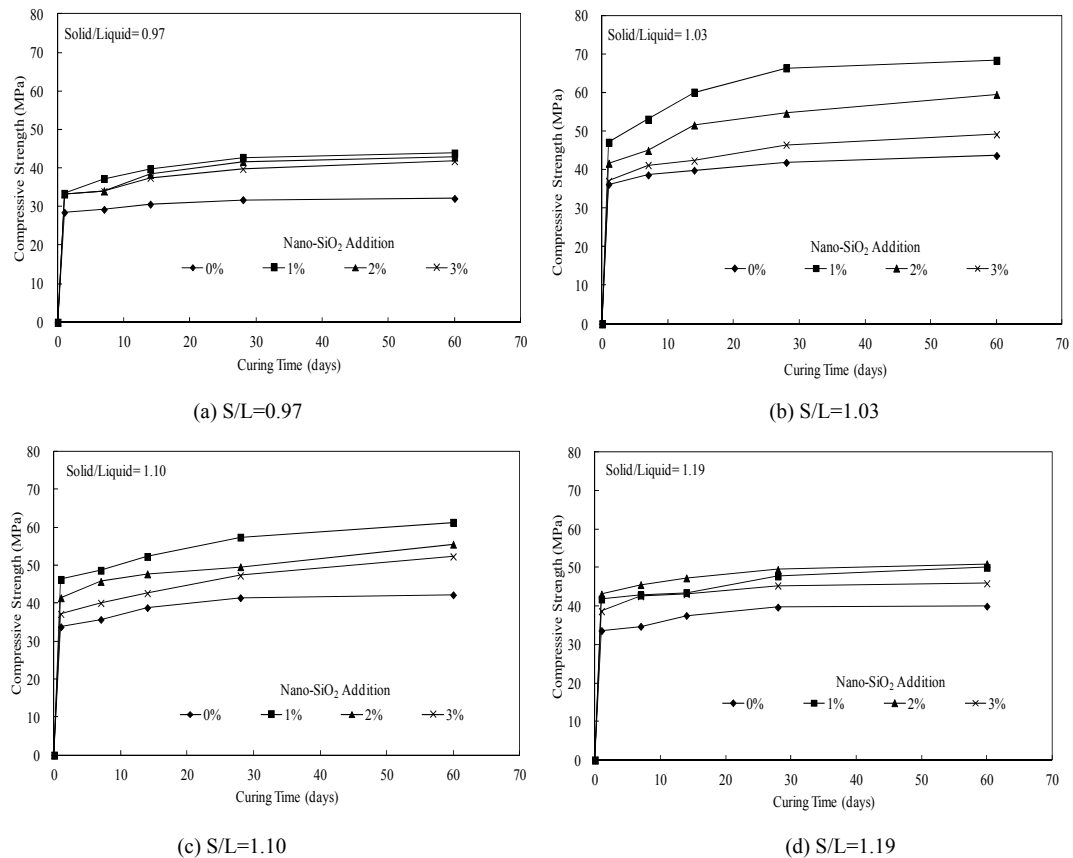


Fig. (2). Initial and final setting time of NS MK-based geopolymers with various S/L ratios.



**Fig. (3).** Compressive strength of NS-MK-based geopolymers with various S/L ratios.

Therefore, insufficient dissolution of Si and Al ions generates too little leading material, producing a low polycondensation level. Parias *et al.* indicated that a relationship exists between polycondensation and the compressive strength of MK geopolymers [16]. When a low S/L ratio was used, there was more fluid medium than solid content in the mixture, and contact between the activating solution and reacting materials was limited because of the large fluid volume. The dissolution of aluminosilicate was slow. This explains the low compressive strength of geopolymers with a S/L ratio of 0.97. By contrast, when a higher S/L ratio was used, the solid content increased. Contact between the activating solution and reacting materials improved and increased the compressive strength [9]. The compressive strength of geopolymers decreased as the solid-to-liquid ratio increased. It is possibly the excessive content of solid in the mixture reduced the workability, the paste hardened sooner, partly unreacted raw materials particles were remained and the reaction process was incomplete, weakening the compressive strength. Therefore, an optimal S/L ratio exists for MK geopolymers. Fig. (3) shows that the compressive strength of the samples increased significantly after adding NS. The best amount of NS is 1% at the S/L ratio from 0.97 to 1.1. It is possibly many unsaturated bonds and different hydroxy bonding state exist in the NS surface, which are in an active and high free-energy state. They would increase the speed and degree of polymerization. In addition, nano particles could fill the paste pore and thus compact the system. This explains why adding NS to the paste improved geopolymer strength. When extra nanoparticles were added,

many unreacted nanoparticles formed nano-interaction energy led to reduced the compressive strength because of their dispersion effect [17].

### 3.3. MIP Results

Polymerization generates geopolymer hydration products. These products increase with the reaction degree, filling holes and making structures denser. According to the IUPAC pore radius classification, pores are classified as micropores, mesopores, macropores, and air voids or cracks. Micropores, mesopores, macropores, and voids or crack apertures are <1 nm, 1 to 25 nm, 25 to 5000 nm, and 5000 to 50 000 nm, respectively [18]. The MIP technique enables a better understanding of the effects of different S/L ratios and NS additions on the connectivity and capacity of the geopolymer pore structure. Fig. (4) shows the cumulative pore volumes of NS MK-based geopolymers at various S/L ratios. The cumulative pore volume of pure MK-based geopolymers was larger, and the distribution range was wide (10 to 100 nm). After adding NS, the cumulative pore volume of the samples decreased significantly, and the more mesopores were observed. When the S/L ratio was 1.03 and 1% NS was added, the cumulative pore volume became denser. As the cumulative pore volume decreases, the paste structure tends toward densification. This is consistent with the compressive strength results.

Fig. (5) shows the pore volume percentage of NS MK-based geopolymers at various S/L ratios. Mesopores were

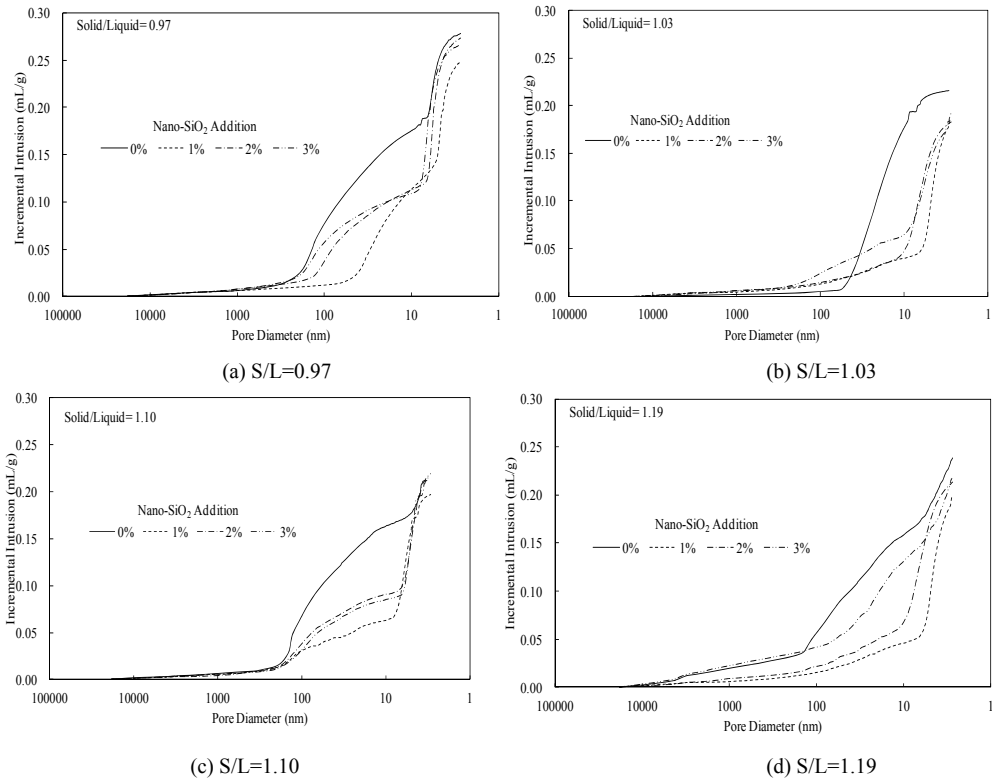


Fig. (4). Cumulative pore volume of NS-MK-based geopolymers with various S/L ratios.

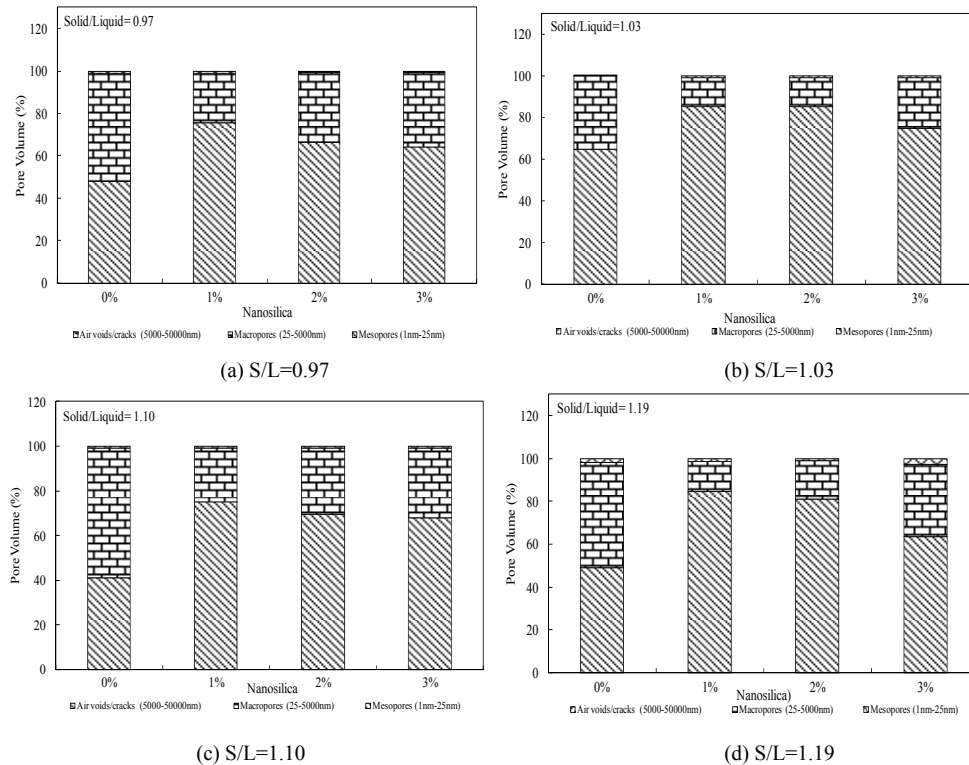
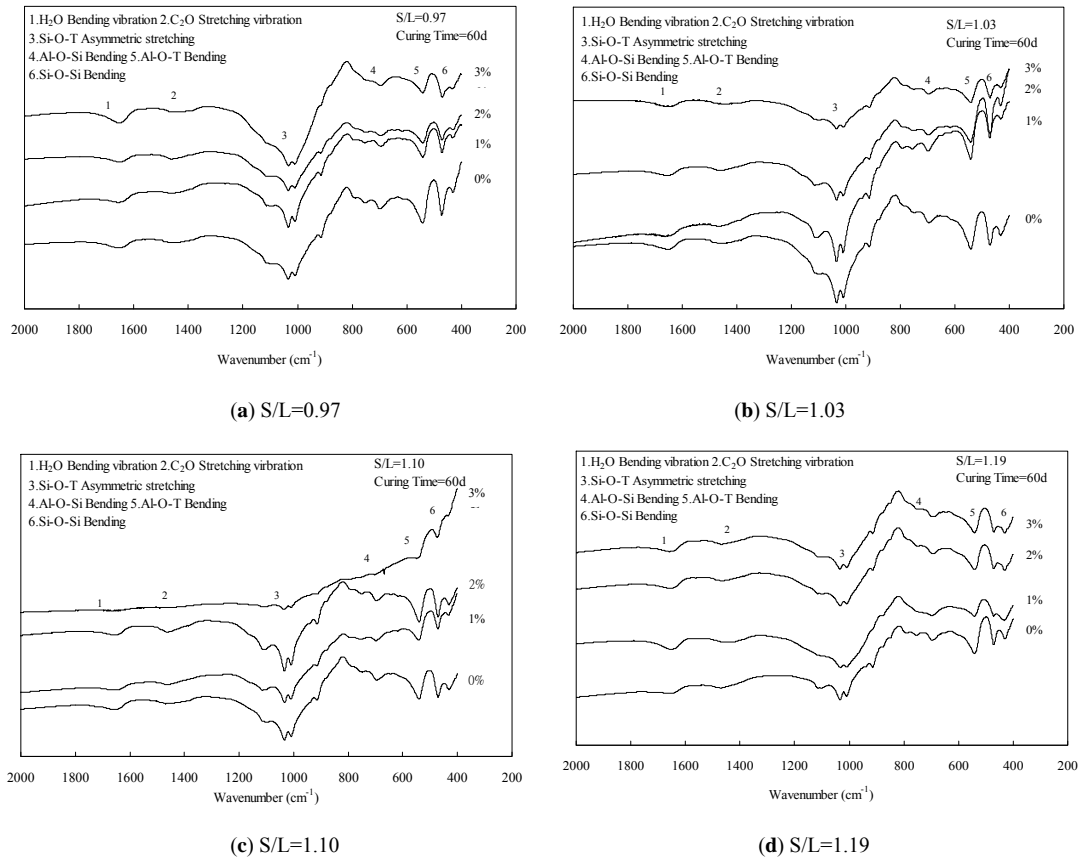


Fig. (5). Percentage of pore volume of NS-MK-based geopolymers with various S/L ratios.

presented in the aluminosilicate gel network. Macropores may transform into mesopores with the polycondensation of hydrated gels and the effects of NS because larger pores are filled with new reaction products. The 1% NS MK-based geopolymer contained more mesopores volumes. The litera-

ture indicated that pores larger than 200 nm in geopolymer pastes were probably associated with interfacial spaces between partially reacted or unreacted raw material and the geopolymer gel [13].



**Fig. (6).** FTIR spectra of NS-MK-based geopolymers with various S/L ratios (Curing Time =60 days).

### 3.4. FTIR Analysis

Fig. (6) shows the FTIR spectra of NS MK-based geopolymers at 60 days. FTIR geopolymer band spectra between 1650 and 1655  $\text{cm}^{-1}$  correspond to OH vibrations. These peaks indicate the presence of weak H<sub>2</sub>O bonds absorbed in the surface or caught in structure cavities [9]. The apparent bond at approximately 470  $\text{cm}^{-1}$  is attributed to Si-O-Si bending. The FTIR spectrum of geopolymer showed a distinct intensity band between 1300 and 900  $\text{cm}^{-1}$  associated with the Si-O-T asymmetric vibration. The Si-O-T vibration was more prominent than the Si-O-Si bending, logical to use the Si-O-T vibration to indicate the degree of geopolymerization [19]. Adsorption at 700  $\text{cm}^{-1}$  is assigned to Si-O-Al bending, showing that the main geopolymer structure generated after the reaction between silicon aluminates and the highly alkali solution was Si-O-Al bending. A weak Al-O-T bending band was observed between 540 and 555  $\text{cm}^{-1}$ . The band at approximately 1460  $\text{cm}^{-1}$  is related to carbonate formation because of alkali metal hydroxide reacting with atmospheric CO<sub>2</sub> [20]. Bands near 800  $\text{cm}^{-1}$  on the spectra for the initial MK (corresponding to the Al(IV)-O vibration band) were also observed [21]. At a higher S/L ratio, this band peak was more obvious, indicating that the geopolymer structure contained unreacted MK. When the S/L ratio was the same, the Si-O-T band changed slightly. The Si-O-T vibration band shifted to lower frequencies as more NS was added. Somna *et al.* noted that the peak shift of the 900 to 1200  $\text{cm}^{-1}$  band was related to the geopolymer Si/Al content [22].

### 3.5. SEM Observation

Fig. (7) shows SEM images of MK-based geopolymers with various S/L ratios (0.97 to 1.19) at 60 days. The micrographs show that the specimens were heterogeneous, some large particles and pores were embedded in the matrix. Many unreacted MK particles which were layered and had angular edges existed in samples with high S/L ratios. For instance, unreacted and flaked MK particles are clearly visible in the SEM images when the S/L ratio is 1.19. When the S/L was relatively low, excess water diluted the colloidal substances generated by the polymerization reaction. More pores were produced, and the structure became looser. The structure of the specimen with the S/L ratio of 1.03 was more compact with fewer unreacted particles. This was consistent with the results of the previous experiment. The MK-based geopolymer with the S/L ratio of 1.03 exhibited the highest compressive strength and lowest porosity.

Fig. (8) reveals the microstructure of NS MK-based geopolymers with the S/L ratio of 1.03 at 60 days. The photographs show many irregular pores. Bubble encapsulation or the contact surface between unreacted particles and the geopolymer generated these pores. The structure became more compact after adding NS because NS would fill the pores. When the S/L ratio was 1.03 and 1% NS was added, the pore volume became denser. As the pore volume decreases, the paste structure tends toward densification. Compared with other samples, the structure with 1% added NS was denser, uniform, flat, and exhibited better cementing ability between particles, which increased the compressive strength. Because

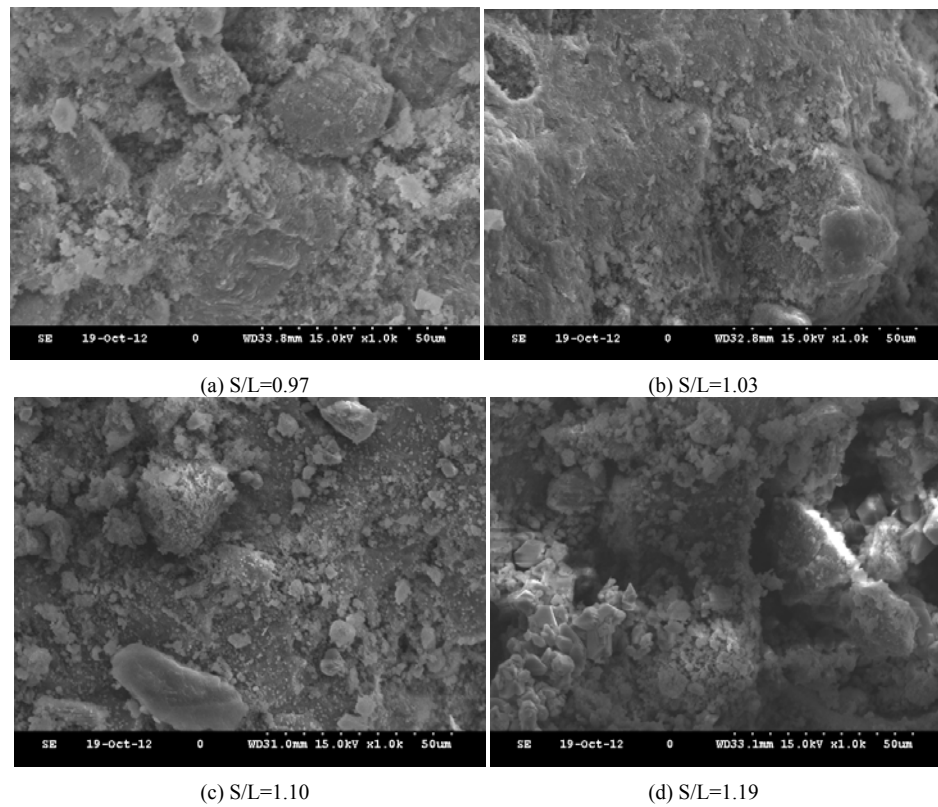


Fig. (7). SEM photographs of MK-based geopolymers with various S/L ratios (Curing time=60 days).

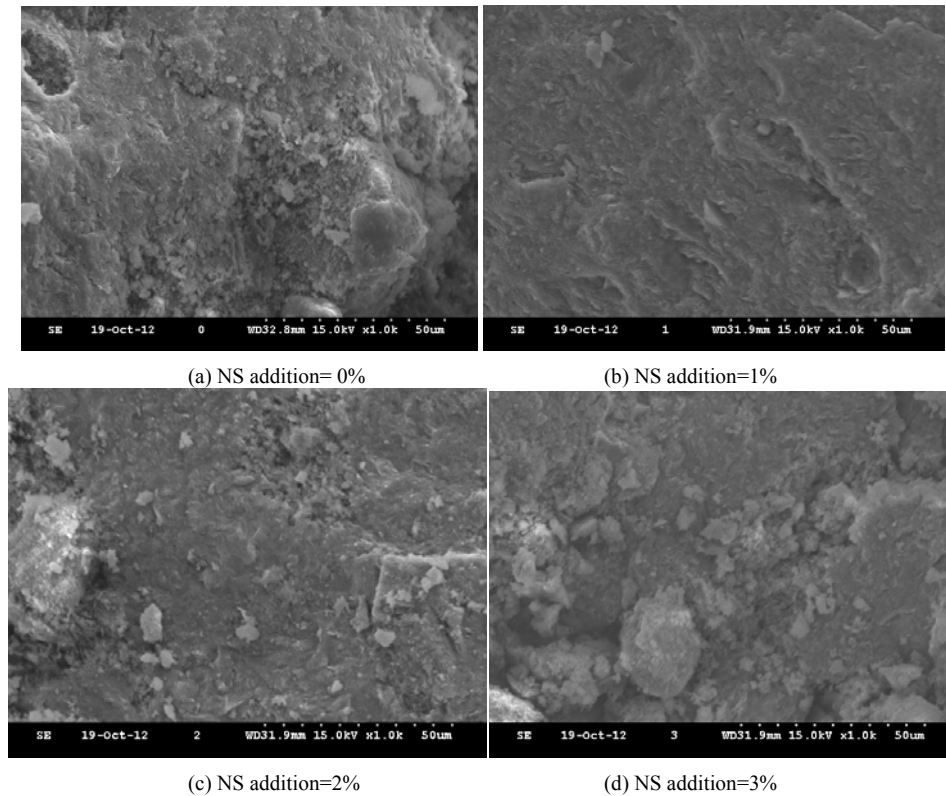


Fig. (8). SEM photographs of MK-based geopolymers with various NS additions.

the excessive NS showed the dispersion effect and did not exhibit gelatination, the structure became looser and strength decreased when 2% and 3% NS were added.

#### 4. CONCLUSIONS

MK-based geopolymers with a S/L ratio of 1.03 and 0.97 produced the highest and lowest compressive strengths, re-

spectively. When the S/L ratio of MK-based geopolymers was 1.03, the optimal NS addition was 1%. At this ratio, the sample exhibited smaller cumulative pore volume and higher mesopores volume percentage. The FTIR spectrum of geopolymer samples contained a distinct intensity band at 1300 to 900  $\text{cm}^{-1}$  associated with the Si-O-T asymmetric vibration. This bond is often used to determine the degree of polymerization. The Si-O-T vibration band shifted to lower frequencies as more NS was added. The setting time of geopolymers decreased with the addition of NS because of the high nanoparticle activity, which promotes the reaction rate. The setting time also decreased with an increase in the S/L ratio. MIP analysis showed that specimens added 1% NS were more compact. These results show the potential for nanotechnology geopolymer applications. As science and technology develop, more nanomaterial will be produced, promoting the application of nanomaterials in geopolymers.

### CONFLICT OF INTEREST

The authors confirm that this article content has no conflicts of interest.

### ACKNOWLEDGEMENT

None declared.

### REFERENCES

- [1] J. Davidovits, "Geopolymers-inorganic polymeric new materials", *J. Therm. Anal.*, vol. 37, pp. 1633-1656, 1991.
- [2] D. Khale, and R. Chaudhary, "Mechanism of geopolymerization and factors influencing its development: a review", *J. Mater. Sci.*, vol. 42, pp. 729-746, 2007.
- [3] G. J. Zheng, X. M. Cui, W. P. Zhang, and F. T. Zhang, "Preparation of geopolymer precursors by sol-gel method and their characterization", *J. Mater. Sci.* 2009; vol. 44, no 15, pp. 3991-3996.
- [4] J. Davidovits, "Geopolymers and geopolymer new materials", *J. Therm. Anal.*, vol. 35, no 2, pp. 429-444, 1989.
- [5] J. G. S. van Jaarsveld, J. S. J. van Deventer, and L. Lorenzen, "The potential use of geopolymer materials to immobilize toxic metals: part I. Theory and applications", *Miner. Eng.*, vol. 10, pp.659-669, 1999.
- [6] Y. S. Zhang, W. Sun, and Z. J. Li, "Composition design and microstructural characterization of calcined kaolin-based geopolymer cement", *Appl. Clay. Sci.*, vol. 47, pp.271-275, 2010.
- [7] D. S. Sun, A. G. Wang, and P. H. Hu, "Geopolymer research and application prospect", *Mater. Rev.*, vol. 7, pp.61-65, 2005. (In Chinese)
- [8] J. L. Provis, P. Duxson, R M. Harrex, C. Z. Yong, and J. S. J. Van Deventer, "Valorisation of fly ashes by geopolymerisation", *Glob. Nest. J.*, vol.11, no. 2; pp. 147-154, 2008.
- [9] C. Y. Heah, H. Kamarudin, A. M. Mustafa, A. Bakri, M. Bhusain, M. Luqman, I. K. Nizar, C. M. Ruzaidi, and Y. M. Liew, "Study on solids-to-liquid and alkaline activator ratios on kaolin-based geopolymers", *Constr. Build. Mater.*, vol. 35, pp. 912-922, 2012.
- [10] F. S. Yang, A. N. Zhou, L. M. Ge, T. L. Li, and J. L. Qu, "Nano technology in polymer modification applications", *Chem. Prog.*, vol. 20, no. 8; pp.9-12, 2001. (In Chinese)
- [11] Y. Zheng, W. H. Xiong, W. J. Liu, W. Lei, and Q. Yuan, "Effect of nano addition on the microstructures and mechanical properties of Ti (C, N)-based cermets", *Ceram. Int.*, vol. 31, no 1: pp. 165-170, 2005.
- [12] M. Aly, M. S. J. Hashmi, A. G. Olabi, M. Messeiry, E. F. Abadir, A. I. Hussain, "Effect of colloidal nano-silica on the mechanical and physical behavior of waste-glass cement mortar", *Mater. Des.*, vol. 33, pp. 127-135, 2012.
- [13] E. D. Rodriguez, S. A. Bernal, J.L. Provis, J. Paya, J. M. Monzo, and M. V. Borrachero, "Effect of nanosilica-based activators on the performance of an alkali-activated fly ash binder", *Cement Concrete Compos.*, vol. 35, pp. 1-11, 2013.
- [14] M. H. Zhang, J. Islam, and S. Peethamparan, "Use of nano-silica to increase early strength and reduce setting time of concretes with high volumes of slag", *Cement Concrete Compos.*, vol. 34, pp.650-662, 2012.
- [15] K. L. Lin, W. C. Chang, D. F. Lin, H. L. Luo, and M. C. Tsai, "Effect of nano-SiO<sub>2</sub> and different ash particle sizes on sludge ash-cement mortar", *J. Environ. Manag.*, vol. 88, pp. 708-714, 2008.
- [16] D. Papias, I. P. Giannopoulou, and T. Perraki, "Effect of synthesis parameters on the mechanical properties of fly ash-based geopolymers", *Colloids Surf. A Physicochem. Eng. Aspects.*, vol. 301, pp. 246-254, 2007.
- [17] W. J. Wang, X. R. Zhu, and P. F. Fang, "Nanosilicon powder cement solidification mechanism research", *J. Zhejiang. Univ.*, vol. 39, no 1, pp.148-153, 2005. (In Chinese)
- [18] D. L. Y. Kong, J. G. Sanjayan, and K. Sagoe-Crentsil, "Comparative performance of geopolymers made with metakaolin and fly ash after exposure to elevated temperatures", *Cement Concrete Compos. Res.*, vol. 37, pp. 1583-1589, 2007.
- [19] P. Chindaprasit, C. Jaturapitakkul, W. Chalee, and U. Rattanasak, "Comparative study on the characteristics of fly ash and bottom ash geopolymers", *Waste Manag.*, vol. 29, pp. 539-543, 2009.
- [20] S. Andini, R. Cioffi, F. Colangelo, T. Grieco, F. Montagnaro, and L. Santoro, "Coal fly ash as raw material for the manufacture of geopolymer-based products", *Waste Manag.*, vol. 28, pp. 416-423, 2008.
- [21] M. L. Granizo, M. T. Blanco-Varela, and A. Palomo, "Influence of the starting kaolin on alkali-activated materials based on metakaolin. Study of the reaction parameters by isothermal conduction calorimetry", *J. Mater. Sci.*, vol. 35, no. 24, pp. 6309-6315, 2000.
- [22] K. Somna, C. Jaturapitakkul, P. Kajitvichyanukul, and P. Chindaprasit, "NaOH-activated ground fly ash geopolymer cured at ambient temperature", *Fuel*, vol. 90, pp. 2118-2124, 2011.

Received: February 18, 2013

Revised: April 21, 2013

Accepted: June 27, 2013

© Gao et al.; Licensee Bentham Open.

This is an open access article licensed under the terms of the Creative Commons Attribution Non-Commercial License (<http://creativecommons.org/licenses/by-nc/3.0/>) which permits unrestricted, non-commercial use, distribution and reproduction in any medium, provided the work is properly cited.